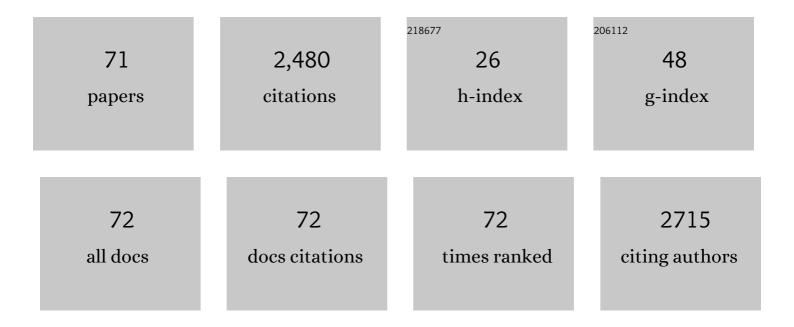
Takazo Shibuya

List of Publications by Year in descending order

Source: https://exaly.com/author-pdf/9746622/publications.pdf Version: 2024-02-01



#	Article	IF	CITATIONS
1	Experimental chondrite–water reactions under reducing and low-temperature hydrothermal conditions: Implications for incipient aqueous alteration in planetesimals. Geochimica Et Cosmochimica Acta, 2022, 319, 151-167.	3.9	6
2	Enceladus as a potential oasis for life: Science goals and investigations for future explorations. Experimental Astronomy, 2022, 54, 809-847.	3.7	5
3	Tellurium stable isotope composition in the surface layer of ferromanganese crusts from two seamounts in the Northwest Pacific Ocean. Geochimica Et Cosmochimica Acta, 2022, 318, 279-291.	3.9	6
4	Heterogeneous nature of the carbonaceous chondrite breccia Aguas Zarcas – Cosmochemical characterization and origin of new carbonaceous chondrite lithologies. Geochimica Et Cosmochimica Acta, 2022, 334, 155-186.	3.9	7
5	Characterization of groundwater chemistry beneath Gale Crater on early Mars by hydrothermal experiments. Icarus, 2022, 386, 115149.	2.5	0
6	The role of hydrothermal sulfate reduction in the sulfur cycles within Europa: Laboratory experiments on sulfate reduction at 100ÂMPa. Icarus, 2021, 357, 114222.	2,5	13
7	Thermodynamic Constraints on Smectite and Iron Oxide Formation at Gale Crater, Mars: Insights into Potential Free Energy from Aerobic Fe Oxidation in Lake Water–Groundwater Mixing Zone. Minerals (Basel, Switzerland), 2021, 11, 341.	2.0	4
8	Stable Abiotic Production of Ammonia from Nitrate in Komatiite-Hosted Hydrothermal Systems in the Hadean and Archean Oceans. Minerals (Basel, Switzerland), 2021, 11, 321.	2.0	10
9	Composition of the Primordial Ocean Just after Its Formation: Constraints from the Reactions between the Primitive Crust and a Strongly Acidic, CO2-Rich Fluid at Elevated Temperatures and Pressures. Minerals (Basel, Switzerland), 2021, 11, 389.	2.0	13
10	Organic matter in carbonaceous chondrite lithologies of Almahata Sitta: Incorporation of previously unsampled carbonaceous chondrite lithologies into ureilitic regolith. Meteoritics and Planetary Science, 2021, 56, 1311-1327.	1.6	5
11	Chemical Nature of Hydrothermal Fluids Generated by Serpentinization and Carbonation of Komatiite: Implications for H ₂ â€Rich Hydrothermal System and Ocean Chemistry in the Early Earth. Geochemistry, Geophysics, Geosystems, 2021, 22, e2021GC009827.	2.5	9
12	Kinetics in thermal evolution of Raman spectra of chondritic organic matter to evaluate thermal history of their parent bodies. Meteoritics and Planetary Science, 2020, 55, .	1.6	5
13	Simulating Serpentinization as It Could Apply to the Emergence of Life Using the JPL Hydrothermal Reactor. Astrobiology, 2020, 20, 307-326.	3.0	22
14	Identification of paleomagnetic remanence carriers in ca. 3.47ÂGa dacite from the Duffer Formation, the Pilbara Craton. Physics of the Earth and Planetary Interiors, 2020, 299, 106411.	1.9	0
15	Experimental and Simulation Efforts in the Astrobiological Exploration of Exooceans. Space Science Reviews, 2020, 216, 9.	8.1	25
16	Chemical assessment of the explosive chamber in the projector system of Hayabusa2 for asteroid sampling. Earth, Planets and Space, 2020, 72, .	2.5	8
17	Experimental Simulations of Hypervelocity Impact Penetration of Asteroids Into the Terrestrial Ocean and Benthic Cratering. Journal of Geophysical Research E: Planets, 2020, 125, e2019JE006291.	3.6	2
18	Peptide Synthesis under the Alkaline Hydrothermal Conditions on Enceladus. ACS Earth and Space Chemistry, 2019, 3, 2559-2568.	2.7	20

Τακάζο Shibuya

#	Article	IF	CITATIONS
19	Enceladus: Evidence and Unsolved Questions for an Ice-Covered Habitable World. , 2019, , 399-407.		1
20	Molecular-scale insights into differences in the adsorption of cesium and selenium on biogenic and abiogenic ferrihydrite. Geochimica Et Cosmochimica Acta, 2019, 251, 1-14.	3.9	19
21	Genomeâ€enabled metabolic reconstruction of dominant chemosynthetic colonizers in deepâ€sea massive sulfide deposits. Environmental Microbiology, 2018, 20, 862-877.	3.8	41
22	Recycled Archean sulfur in the mantle wedge of the Mariana Forearc and microbial sulfate reduction within an extremely alkaline serpentine seamount. Earth and Planetary Science Letters, 2018, 491, 109-120.	4.4	14
23	Ar–Ar dating for hydrothermal quartz from the 2.4 Ga Ongeluk Formation, South Africa: implications for seafloor hydrothermal circulation. Royal Society Open Science, 2018, 5, 180260.	2.4	0
24	Biological and physical modification of carbonate system parameters along the salinity gradient in shallow hypersaline solar salterns in Trapani, Italy. Geochimica Et Cosmochimica Acta, 2017, 208, 354-367.	3.9	15
25	Europium anomaly variation under low-temperature water-rock interaction: A new thermometer. Geochemistry International, 2017, 55, 822-832.	0.7	15
26	Deepest and hottest hydrothermal activity in the Okinawa Trough: the Yokosuka site at Yaeyama Knoll. Royal Society Open Science, 2017, 4, 171570.	2.4	48
27	Weak hydrothermal carbonation of the Ongeluk volcanics: evidence for low CO2 concentrations in seawater and atmosphere during the Paleoproterozoic global glaciation. Progress in Earth and Planetary Science, 2017, 4, .	3.0	6
28	Removal of organic contaminants from iron sulfides as a pretreatment for mineral-mediated chemical synthesis under prebiotic hydrothermal conditions. Geochemical Journal, 2017, 51, 495-505.	1.0	3
29	Reactions between komatiite and CO2-rich seawater at 250 and 350°C, 500 bars: implications for hydrogen generation in the Hadean seafloor hydrothermal system. Progress in Earth and Planetary Science, 2016, 3, .	3.0	24
30	Rapid growth of mineral deposits at artificial seafloor hydrothermal vents. Scientific Reports, 2016, 6, 22163.	3.3	44
31	Fluid chemistry in the Solitaire and Dodo hydrothermal fields of the Central Indian Ridge. Geofluids, 2016, 16, 988-1005.	0.7	29
32	PIXE and microthermometric analyses of fluid inclusions in hydrothermal quartz from the 2.2Ga Ongeluk Formation, South Africa: Implications for ancient seawater salinity. Precambrian Research, 2016, 286, 337-351.	2.7	7
33	Free energy distribution and hydrothermal mineral precipitation in Hadean submarine alkaline vent systems: Importance of iron redox reactions under anoxic conditions. Geochimica Et Cosmochimica Acta, 2016, 175, 1-19.	3.9	52
34	Authigenic carbonate precipitation at the end-Guadalupian (Middle Permian) in China: Implications for the carbon cycle in ancient anoxic oceans. Progress in Earth and Planetary Science, 2015, 2, .	3.0	11
35	Hydrogen-rich hydrothermal environments in the Hadean ocean inferred from serpentinization of komatiites at 300°C and 500Âbar. Progress in Earth and Planetary Science, 2015, 2, .	3.0	45
36	Rock magnetism of tiny exsolved magnetite in plagioclase from a Paleoarchean granitoid in the Pilbara craton. Geochemistry, Geophysics, Geosystems, 2015, 16, 112-125.	2.5	20

Τακάζο Shibuya

#	Article	IF	CITATIONS
37	In-situ iron isotope analyses of pyrites from 3.5 to 3.2Ga sedimentary rocks of the Barberton Greenstone Belt, Kaapvaal Craton. Chemical Geology, 2015, 403, 58-73.	3.3	17
38	Ongoing hydrothermal activities within Enceladus. Nature, 2015, 519, 207-210.	27.8	382
39	Potential for biogeochemical cycling of sulfur, iron and carbon within massive sulfide deposits below the seafloor. Environmental Microbiology, 2015, 17, 1817-1835.	3.8	42
40	High-temperature water–rock interactions and hydrothermal environments in the chondrite-like core of Enceladus. Nature Communications, 2015, 6, 8604.	12.8	152
41	Petrology of Peridotites and Related Gabbroic Rocks Around the Kairei Hydrothermal Field in the Central Indian Ridge. , 2015, , 177-193.		4
42	Development of Hydrothermal and Frictional Experimental Systems to Simulate Sub-seafloor Water–Rock–Microbe Interactions. , 2015, , 71-85.		2
43	Experimental Hydrogen Production in Hydrothermal and Fault Systems: Significance for Habitability of Subseafloor H2 Chemoautotroph Microbial Ecosystems. , 2015, , 87-94.		1
44	The Drive to Life on Wet and Icy Worlds. Astrobiology, 2014, 14, 308-343.	3.0	232
45	Diversity of fluid geochemistry affected by processes during fluid upwelling in active hydrothermal fields in the Izena Hole, the middle Okinawa Trough back-arc basin. Geochemical Journal, 2014, 48, 357-369.	1.0	69
46	Exploration of Enceladus^ ^apos; Water-Rich Plumes toward Understanding of Chemistry and Biology of the Interior Ocean. Transactions of the Japan Society for Aeronautical and Space Sciences Aerospace Technology Japan, 2014, 12, Tk_7-Tk_11.	0.2	5
47	Reactions between basalt and CO2-rich seawater at 250 and 350 ŰC, 500 bars: Implications for the CO2 sequestration into the modern oceanic crust and the composition of hydrothermal vent fluid in the CO2-rich early ocean. Chemical Geology, 2013, 359, 1-9.	3.3	56
48	Nitrification-driven forms of nitrogen metabolism in microbial mat communities thriving along an ammonium-enriched subsurface geothermal stream. Geochimica Et Cosmochimica Acta, 2013, 113, 152-173.	3.9	23
49	Decrease of seawater CO2 concentration in the Late Archean: An implication from 2.6 Ga seafloor hydrothermal alteration. Precambrian Research, 2013, 236, 59-64.	2.7	16
50	Elemental dissolution of basalts with ultra-pure water at 340°C and 40 Mpa in a newly developed flow-type hydrothermal apparatus. Geochemical Journal, 2013, 47, 89-92.	1.0	3
51	Petrogenesis of the ridge subduction-related granitoids from the Taitao Peninsula, Chile Triple Junction Area. Geochemical Journal, 2013, 47, 167-183.	1.0	15
52	Postâ€drilling changes in fluid discharge pattern, mineral deposition, and fluid chemistry in the lheya North hydrothermal field, Okinawa Trough. Geochemistry, Geophysics, Geosystems, 2013, 14, 4774-4790.	2.5	52
53	Chemical composition and K–Ar age of Phengite from Barrovian metapelites, Loch Leven, Scotland. Journal of the Geological Society of Japan, 2013, 119, 437-442.	0.6	2
54	Post-drilling changes in fluid discharge pattern, mineral deposition, and fluid chemistry in the Iheya North hydrothermal field, Okinawa Trough. Geochemistry, Geophysics, Geosystems, 2013, 14, n/a-n/a.	2.5	1

Τακάζο Shibuya

#	Article	IF	CITATIONS
55	Depth variation of carbon and oxygen isotopes of calcites in Archean altered upperoceanic crust: Implications for the CO2 flux from ocean to oceanic crust in the Archean. Earth and Planetary Science Letters, 2012, 321-322, 64-73.	4.4	27
56	Discovery of New Hydrothermal Activity and Chemosynthetic Fauna on the Central Indian Ridge at 18°–20°S. PLoS ONE, 2012, 7, e32965.	2.5	83
57	Monazite geochronology and geochemistry of meta-sediments in the Narryer Gneiss Complex, Western Australia: constraints on the tectonothermal history and provenance. Contributions To Mineralogy and Petrology, 2010, 160, 803-823.	3.1	32
58	Stratigraphy-related, low-pressure metamorphism in the Hardey Syncline, Hamersley Province, Western Australia. Gondwana Research, 2010, 18, 213-221.	6.0	15
59	Grain-scale iron isotopic distribution of pyrite from Precambrian shallow marine carbonate revealed by a femtosecond laser ablation multicollector ICP-MS technique: Possible proxy for the redox state of ancient seawater. Geochimica Et Cosmochimica Acta, 2010, 74, 2760-2778.	3.9	59
60	87Sr/86Sr chemostratigraphy of Neoproterozoic Dalradian carbonates below the Port Askaig Glaciogenic Formation, Scotland. Precambrian Research, 2010, 179, 150-164.	2.7	37
61	Highly alkaline, high-temperature hydrothermal fluids in the early Archean ocean. Precambrian Research, 2010, 182, 230-238.	2.7	88
62	Are the Taitao granites formed due to subduction of the Chile ridge?. Lithos, 2009, 113, 246-258.	1.4	46
63	Variability in Microbial Communities in Black Smoker Chimneys at the NW Caldera Vent Field, Brothers Volcano, Kermadec Arc. Geomicrobiology Journal, 2009, 26, 552-569.	2.0	46
64	H2 generation by experimental hydrothermal alteration of komatiitic glass at 300°C and 500 bars: A preliminary result from on-going experiment. Geochemical Journal, 2009, 43, e17-e22.	1.0	30
65	The youngest blueschist belt in SW Japan: implication for the exhumation of the Cretaceous Sanbagawa highâ€ <i>P/T</i> metamorphic belt. Journal of Metamorphic Geology, 2008, 26, 583-602.	3.4	63
66	Geological background of the Kairei and Edmond hydrothermal fields along the Central Indian Ridge: Implications of their vent fluids' distinct chemistry. Geofluids, 2008, 8, 239-251.	0.7	112
67	Evolution of the composition of seawater through geologic time, and its influence on the evolution of life. Gondwana Research, 2008, 14, 159-174.	6.0	91
68	Large P–T gap between Ballantrae blueschist/garnet pyroxenite and surrounding ophiolite, southern Scotland, UK: Diapiric exhumation of a Caledonian serpentinite mélange. Lithos, 2008, 104, 337-354.	1.4	14
69	Geotectonic framework of the Blueschist Unit on Anglesey–Lleyn, UK, and its role in the development of a Neoproterozoic accretionary orogen. Precambrian Research, 2007, 153, 11-28.	2.7	45
70	Middle Archean ocean ridge hydrothermal metamorphism and alteration recorded in the Cleaverville area, Pilbara Craton, Western Australia. Journal of Metamorphic Geology, 2007, 25, 751-767.	3.4	42
71	Progressive metamorphism of the Taitao ophiolite; evidence for axial and off-axis hydrothermal alterations. Lithos, 2007, 98, 233-260.	1.4	21